The Cerebellum
https://doi.org/10.1007/s12311-022-01430-3

ORIGINAL ARTICLE

Clinical and Molecular Findings of Autosomal Recessive Spastic Ataxia of Charlevoix Saguenay: an Iranian Case Series Expanding the Genetic and Neuroimaging Spectra

Mahmoud Reza Ashrafi[1,2] · Pouria Mohammadi[1,3] · Ali Reza Tavasoli[1,4,5] · Morteza Heidari[1,4] · Sareh Hosseinpour[1,6] · Maryam Rasulinejad[1] · Mohammad Rohani[7] · Masoud Ghahvechi Akbari[1,8] · Reza Azizi Malamiri[9] · Reza Shervin Badv[1] · Davood Fathi[10,11] · Ali Zare Dehnavi[1] · Shahram Savad[12] · Ali Rabbani[1,2] · Matthis Synofzik[13,14] · Nejat Mahdieh[15] · Zahra Rezaei[1]

Accepted: 6 June 2022

Abstract

Autosomal recessive spastic ataxia of Charlevoix Saguenay (ARSACS) is now increasingly identified from all countries over the world, possibly rendering it one of the most common autosomal recessive ataxias. Here, we selected patients harboring *SACS* variants, the causative gene for ARSACS, in a large cohort of 137 patients with early-onset ataxia recruited from May 2019 to May 2021 and were referred to the ataxia clinic. Genetic studies were performed for 111 out of 137 patients (81%) which led to a diagnostic rate of 72.9% (81 out of 111 cases). Ten patients with the molecular diagnosis of ARSACS were identified. We investigated the phenotypic and imaging spectra of all confirmed patients with ARSACS. We also estimated the frequency of ARSACS in this cohort and described their clinical and genetic findings including seven novel variants as well as novel neuroimaging findings. While the classic clinical triad of ARSACS is progressive cerebellar ataxia, spasticity, and sensorimotor polyneuropathy, it is not a constant feature in all patients. Sensorimotor axonal-demyelinating neuropathy was detected in all of our patients, but spasticity and extensor plantar reflex were absent in 50% (5/10). In all patients, brain magnetic resonance imaging (MRI) showed symmetric linear hypointensities in the pons (pontine stripes) and anterior superior cerebellar atrophy as well as a hyperintense rim around the thalami (thalamic rim). Although infratentorial arachnoid cyst has been reported in ARSACS earlier, we report anterior temporal arachnoid cyst in two patients for the first time, indicating that arachnoid cyst may be an associated imaging feature of ARSACS. We also extended molecular spectrum of ARSACS by presenting 8 pathogenic and one variant of unknown significance (VUS) sequence variants, which 7 of them have not been reported previously. MetaDome server confirmed that the identified VUS variant was in the intolerant regions of sacsin protein encoded by *SACS*.

Keywords Spastic ataxia · ARSACS · Mutation · Ataxia of Charlevoix Saguenay

Introduction

Autosomal recessive spastic ataxia of Charlevoix–Saguenay (ARSACS) (OMIM# 270,550) affects almost 5% of patients with recessive spinocerebellar ataxia in population. Historically, ARSACS was being considered as a rare hereditary neurologic disease and as a cause of early-onset ataxia (EOA), means by age of disease onset before 30 years, and was assumed to be restricted to Quebec and French ancestors for a long time. However, it is now increasingly diagnosed so that is being remarked as the second most common cause of recessive early-onset cerebellar ataxia following Friedreich's ataxia worldwide [1–3]. The classic phenotype of ARSACS

Mahmoud Reza Ashrafi and Pouria Mohammadi have an equal contribution as the first authors.

✉ Nejat Mahdieh
nmahdieh@gmail.com

✉ Zahra Rezaei
zahra.rezaii84@gmail.com

Extended author information available on the last page of the article

Published online: 22 June 2022

is characterized by a triad of slowly progressive cerebellar ataxia, spasticity, and sensorimotor axonal-demyelinating polyneuropathy. Some patients may show unusual presentations such as Charcot-Marie-Tooth-like phenotype [2]. Additional complicating clinical features include intellectual disability, urinary, visual or auditory problems, muscle weakness or cramp, and myoclonic epilepsy [4, 5]. Brain magnetic resonance imaging (MRI) typically reveals superior vermal cerebellar atrophy, T2-weighted hypointensity in the pons, or pontine stripes, a hyperintense rim seen on lateral side of the pons, and a T2-w hyperintense rim around the thalami that is known as thalamic rim [6]. Other uncommon MRI findings such as cerebellar hemisphere asymmetry, posterior fossa arachnoid cyst, and Chiari type 1-like malformation have also been reported [2, 5].

SACS gene is highly expressed in the brain, cerebellar Purkinje cells, precerebellar nuclei, corticospinal tract, and cranial motor neurons. Degeneration of cerebellar Purkinje cells and corticospinal tract, as well as peripheral nerve axons, has been reported in patients with ARSACS [7, 8]. Sacsin protein, encoded by the *SACS* gene, has 4,579 amino acids in its canonical isoform and contains N-terminal ubiquitin-like domain (UBL) (amino acid position, 9–84), which mediates interaction with the proteasome components, J domain (amino acid position, 4306–4393) which is functional and is shown to stimulate *E. coli* dnaK ATPase activity, and HEPN domain (amino acid position, 4451–4567) [7, 9]. To date, more than 300 variants have been reported in *SACS* gene based on HGMD database (http://www.hgmd.cf.ac.uk/).

So far, only one Iranian family with molecular diagnosis of ARSACS has been reported [5]. The current study was conducted to investigate the frequency and phenotypic and genotypic spectra of patients with ARSACS in an Iranian cohort of 137 cases with early-onset ataxia. We explicated clinical, laboratory, imaging, electrodiagnostic, and molecular findings of 10 out of 137 cases who met the diagnosis of ARSACS.

Materials and Methods

Study Design and Ethical Considerations

This cohort originated from a national study that was conducted in the context of an international collaboration with the Ataxia Research Group, Hertie-Institute for the Clinical Brain Research, Tübingen, Germany. For all referred patients with early-onset ataxia to the Ataxia clinic at Children's Medical Center, Tehran, Iran, clinical and paraclinical data were recorded using a standard prepared questionnaire. Standard neurological examination tests were applied to the evaluation of cerebellar function in all patients including gait and speech evaluation, dysdiadochokinesia, gaze evaluation, finger to nose and heel to shin tests, and muscle tone and cognition assessment. The severity of ataxia was graded using Scale for Assessment and Rating of Ataxia (SARA) test. Secondary causes of ataxia were excluded by appropriate laboratory investigations including serum electrolytes, serum vitamins E and B12 levels, immunoglobulin levels, alpha-fetoprotein, albumin, liver, kidney, and thyroid function tests, and complete blood count. Lead and copper plasma levels were requested as needed. Electrodiagnostic study and brain magnetic resonance imaging (MRI) including T1-W, T2-W, fluid-attenuated inversion recovery (FLAIR), diffusion-weighted imaging (DWI), and apparent diffusion coefficient (ADC) sequences were performed for all patients. Additional workup such as ophthalmoscopy, audiometry, orthopedic, urologic, or cardiology consults was conducted according to the clinical presentations and neurological examination findings. Lastly, appropriate molecular test was applied individually based on primary clinical presentation, laboratory tests results, and an expert-panel consensus. The molecular tests included targeted gene sequencing for *SACS* plus its splicing regions, triplet repeat primed polymerase change reaction (TP-PCR) for trinucleotide repeat disorders (e.g., Friedreich ataxia), and whole-exome sequencing (WES). Whole-genome sequencing (WGS) were considered for those patients whose WES result was inconclusive. The relevant data of patients harboring mutation in *SACS* were investigated in details. All families and patients were informed about the aims of the study, and informed consent was obtained from patients or their legal guardians. The study was approved by the ethics committee of the National Institute for Medical Research Development (NIMAD) of Iran under the code of ID, IR.NIMAD.REC.1397.508, and has thus been performed in accordance with the ethical standards laid down in the 1964 Declaration of Helsinki and its later amendments.

Whole-Exome Sequencing and Bioinformatics Analysis

DNA was extracted from whole blood using the standard salting-out method. Due to the large exon of the targeted gene, *SACS*, WES by an Illumina HiSeq 4000 platform was performed to identify its variants, and targeted regions were sequenced with at least a read of 100×. The purposed regions were amplified using SimpliAmp™ Thermal Cycler (Thermo Fisher Scientific, USA); briefly, a total volume of 25-µL PCR reactions was used including 10×buffer, 1.5 mM/L MgCl2, 200 mM/L dNTP, 10 pM/L primers, 100 ng of DNA, and 1 U of Taq DNA polymerase (Amplicon, UK). The PCR program was as follows: 94 °C for 5 min 30 cycles of denaturation at 94° C for 30 s, annealing at 62 °C for 30 s, and extension at 72 °C for 30 s. Direct

sequencing was done by the ABI Sequencer 3500XL PE (Applied Bio Systems, USA) [10].

Based on similar studies, bioinformatics tools were used to analyze the WES [11, 12]. Briefly, the Fast P tool was used to check quality control (QC) of reads based on GC content and Phred score value [13]. Burrows–Wheeler Aligner (BWA) aligning tool was recruited to align the sequence reads to the (GRCh38/hg38) human reference genome [14]. Post-alignment QC was performed based on the Picard command-line tools. Genome analysis toolkit Haplotypecaller (GATK HC) and DeepVariant were used to call both single nucleotide (SNV) and insertion/deletion (indel) variants, and then Ensembl variant effect predictor (VEP) was utilized to annotate variant call format (VCF) files.

The R programming command-line software (version 4.1.1) was used to filter the annotated VCFs. First, variants with minor allele frequency (MAF) > 1% were excluded based on genomic population projects such as GnomAD (version:3.1.2), ESP, ExAC, 1000Genome project, and Iranome [15]. In the next step, the remaining variants were filtered based on their consequence, and we focused on coding variants. Then according to the human phenotype ontology (HPO) terms, variants that were not related to the phenotypes were excluded. The remaining variants were classified according to ACMG recommendations [10].

Segregation Analysis and In Silico *Prediction*

Sanger sequencing Applied Biosystems 3130 Genetic Analyzer was utilized to confirm identified sequence variants in patients and to segregate analysis in the family. Primers were designed by the PrimerQuest, and PCR amplification for the region harboring the identified variants was performed. Codoncode aligner software was used for the analysis of Sanger sequencing results. Functional domains and regions of the Sacsin protein were identified by UniProt, ConSurf server. Mutationtaster, FATHMM-MKL, and EIGEN computational predicting tools were used to evaluate the probable effects of the variants [16, 17].

Results

In this cohort, 137 patients with the clinical phenotype of EOA were enrolled from May 2019 to May 2021. Genetic tests include screening for *SACS* which were performed in 111 out of 137 (81%) patients which led to a molecular diagnosis in 81 patients and a diagnostic rate of 72.9%. In 26 patients, genetic tests were not performed due to irregular follow-up. These genetic tests encompassed targeted sequencing for *SACS* and its splicing regions in five cases, TP-PCR in 5 cases, and WES in 101 patients. WES resulted in a molecular diagnosis in 67 patients including 5 cases with ARSACS. At the time of study publication, WGS results were available in 10 out of 34 patients with negative WES analysis, which was conclusive in 4 patients. None of these four patients had ARSACS. Of note, the clinical and imaging findings of all our negative WES patients were not compatible with ARSACS. Overall, ten patients with a sequence variant in *SACS* were detected with WES and targeted sequencing yielding a frequency of 9% (10/111) in an inbreed population of Iranian patients with EOA (Fig. 1). In these ten distinct patients harboring *SACS* variants, genetic test results analysis revealed nine distinguished variants including 8 pathogenic variants and one variant of uncertain significance (VUS). One homozygous pathogenic variant was shared by two patients.

Clinical Findings

Ten patients including five males and five females were diagnosed with ARSACS. The mean age of disease onset was 4.7 years (range, 2–11 years), whereas the mean age of patients was 20.3 years (range, 5–35 years). All patients were born to a consanguineous couple. Family history of similar phenotype was detected in only one patient. Motor milestone achievement was normal in 70% (7/10) of patients. Gait problem was the most common presenting sign detected in all ten patients. In addition, on neurological examination, limbs and gait ataxia as well as impaired cerebellar function tests were the most common findings (10/10, 100%), followed by pyramidal signs (9/10, 90%). All cases experienced a slowly progressive gross motor function deterioration, but their cognitive performance was normal at the time of study. Additionally, mood disorder, upper limb spasticity, slow saccadic eye movement, lower limb joints deformity, and macular pigmentary changes were other uncommon findings among patients. These data are presented in supplementary Table 1. As neuropathy is a common presentation in ARSCS patients, all cases were evaluated by electrodiagnostic study. Primary or secondary axonal neuropathy was found in all patients (10/10, 100%). Basic laboratory study was normal in all cases. Atrophy of superior cerebellar vermis, pontine stripes, and thalamic rim were the most frequent imaging findings. Posterior fossa arachnoid cyst was detected in 5 patients, however; anterior temporal arachnoid cyst was also detected in two additional cases. Notably, arachnoid cyst was detected in 9.6% of all enrolled patients with early-onset ataxia other than ARSACS. The main clinical, laboratory, and electrodiagnostic data as well as MRI findings of patients are summarized in Tables 1 and 2, respectively. Figure 2 also depicts significant imaging findings of our patients.

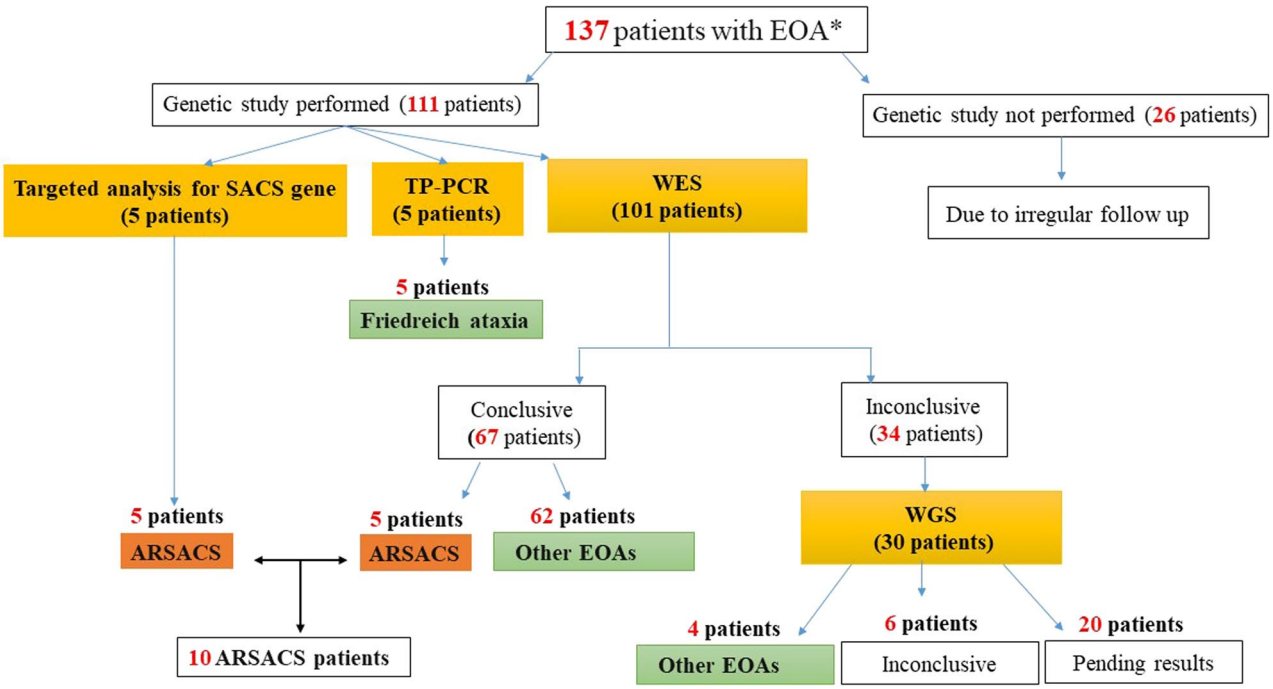

Fig. 1 Flow chart of the cohort with ten patients with ARSAC

Exome Sequencing Results and Segregation Analysis

According to the American College of Medical Genetics (ACMG), nine distinct variants were identified in the *SACS* gene with WES and targeted sequencing of SCAS, and its splicing regions met the criteria of being pathogenic for 8 and VUS for one sequence variants. Although WGS was performed for 30 out of 34 patients with negative WES results, none of the reported SACS variants were detected by WGS. These variants included six homozygous nonsense variants in 6 patients, [patient A, NM_014363.6: c.10813A > T; (p.Lys3605Ter)], [patient B, NM_014363.6; c.9866C > G; (p.Ser3289Ter)], [patient C, NM_014363.6: c.8132C > A; (p.Ser2711Ter)], [patient F, NM_014363.6: c.3427C > T; (p.Gln1143Ter)], [patient G, NM_014363.6: c.8716C > T; (p.Arg2906Ter)], and [patient H, NM_014363.6: c.7504C > T; (p.Arg2502Ter)], which cause premature stop codons in the *SACS* gene; two frameshift variants in 3 patients, [patient D, NM_014363.6: c.2439_2440delAT; (p.Val815GlyfsTer4)] and [patients E and I, NM_014363.6: c.3281dupA; (p.Asn1094LysfsTer18)]; and one inframe deletion VUS variant in one patient [patient J, NM_014363.6: c.3695_3697del; (p.Val1232del)]. Seven of these variants are unreported based on HGMD database (identified variants in the patients A, B, C, E and I, F, G, and J), and two of them had previously been reported (identified variants in the patients D and H). The characteristics of all these sequence variants are summarized in Table 3. Pathogenic variants in the *SACS* gene are consistent with ARSACS [18]. The identified variants were confirmed by Sanger sequencing and segregated with the disease in the families. Mapping of sequence variants in our patients on *SACS* gene has been illustrated in Fig. 3A. All identified variants were located in exon 10 of the *SACS* gene, including eight pathogenic variants shown in black and one VUS variant shown in red. Graphical view of the Sacsin protein (UniProtKB, Q9NZJ4) updated from UniProt (https://www.uniprot.org/uniprot/Q9NZJ4) has been also demonstrated in Fig. 3B. The canonical isoform length of the Sacsin protein (identifier, Q9NZJ4-1) has 4579 amino acids and contains three functional domains, including ubiquitin-like domain (UBL) (residue 9–84), J domain (residue 4306–4393), and HEPN domain (residue 4451–4567). MetaDome server (https://stuart.radboudumc.nl/metadome) was used to identify the intolerant regions in the sacsin protein for the identified VUS variant in this study. As shown by the red arrow, Val1232 is located in a highly intolerant region of the protein.

Discussion

The present study determined ARSACS as a common cause of early-onset ataxia, while it was diagnosed genetically in 9% (10/111) of enrolled cases in this cohort. A

Table 1 Main clinical and paraclinic findings of the patients

Patient ID	Age of onset[1]	Age of evaluation	Limb ataxia[2]	Gait ataxia	Dysarthria	Extension plantar response	Lower limb spasticity	SARA[3]	Electrodiagnosis[4]	Laboratory evaluation[5,6]
A	10	27	+	++	-	-	-	5	D/secondary A	Nl
B	11	35	+	++	+	+	+	7	D/secondary A	Nl
C	7	18	+	++	+	+	-	10	D/secondary A	Nl
D	5	17	+	++	+	+	+	6	A	Nl
E	2	11	++	++	+	-	+	12	A	Nl
F	3	8	++	++	-	+	+	11	D/secondary A	Nl
G	2	11	++	++	-	+	-	6	A	Nl
H	2	31	+	++	-	-	+	20	A	Nl
I	2	5	++	++	+	-	+	10	A	Nl
J	3	10	+	++	+	-	+	10	D/secondary A	Nl

[1]Age is measured by year

[2]Limb ataxia contains of dysmetria, dyssynergia, and intention tremor. It is clinically assessed by the finger-to-nose and heel-to-knee tests

[3]*SARA*, Scale for the Assessment and Rating of Ataxia

[4]*D*, demyelinating; *A*, axonal

[5]Basic laboratory evaluation (performed for all patients): electrolytes, vitamin E and B12 level, immunoglobulin levels, alpha-fetoprotein, albumin, liver/kidney, and thyroid function tests, complete blood count, lead and copper plasma level

[6]Clinical manifestations not detected in any patient: intellectual disability, urinary dysfunction, hearing problem, muscle weakness, dysphagia, dystonia, seizure, school performance dysfunction

Symptom severity: +, mild; ++, moderate; +++, severe

Table 2 MRI findings of patients with ARSACS

	MRI findings	Patients*								
		A	B	C	D	E	F	H	I	J
1	Atrophy of the superior cerebellar vermis	✓	✓	✓	✓	✓	✓	✓	✓	✓
2	Thinning of the posterior mid-body of the corpus callosum	✓	✓	✓	✓	✓	✓	-	-	✓
3	Bilateral hypointense stripes in the pons on T2/ FLAIR sequences	✓	✓	✓	✓	✓	✓	✓	✓	✓
4	Bilateral hyperintensity of the lateral pons/MCP on coronal T2-w sequence	✓	✓	-	✓	✓	✓	✓	✓	✓
5	Hyperintense rim around both thalami on T2-w sequence	✓	✓	✓	✓	✓	✓	✓	✓	✓
6	Bilateral parietal atrophy on T1-w sequence	-	-	-	-	-	-	-	-	✓
7	Arachnoid cyst of post fossa	-	-	-	✓	✓	✓	✓	✓	-
8	Thickening of middle cerebellar peduncle	✓	-	-	✓	-	-	-	-	✓
9	Asymmetry of cerebellar hemispheres	-	-	-	-	✓	-	-	-	-
10	Temporal arachnoid cyst	-	-	✓	✓	-	-	-	-	-

*For patient G, most parts of brain MRI data were not available at the time of the study; therefore, this patient was excluded from Table 2

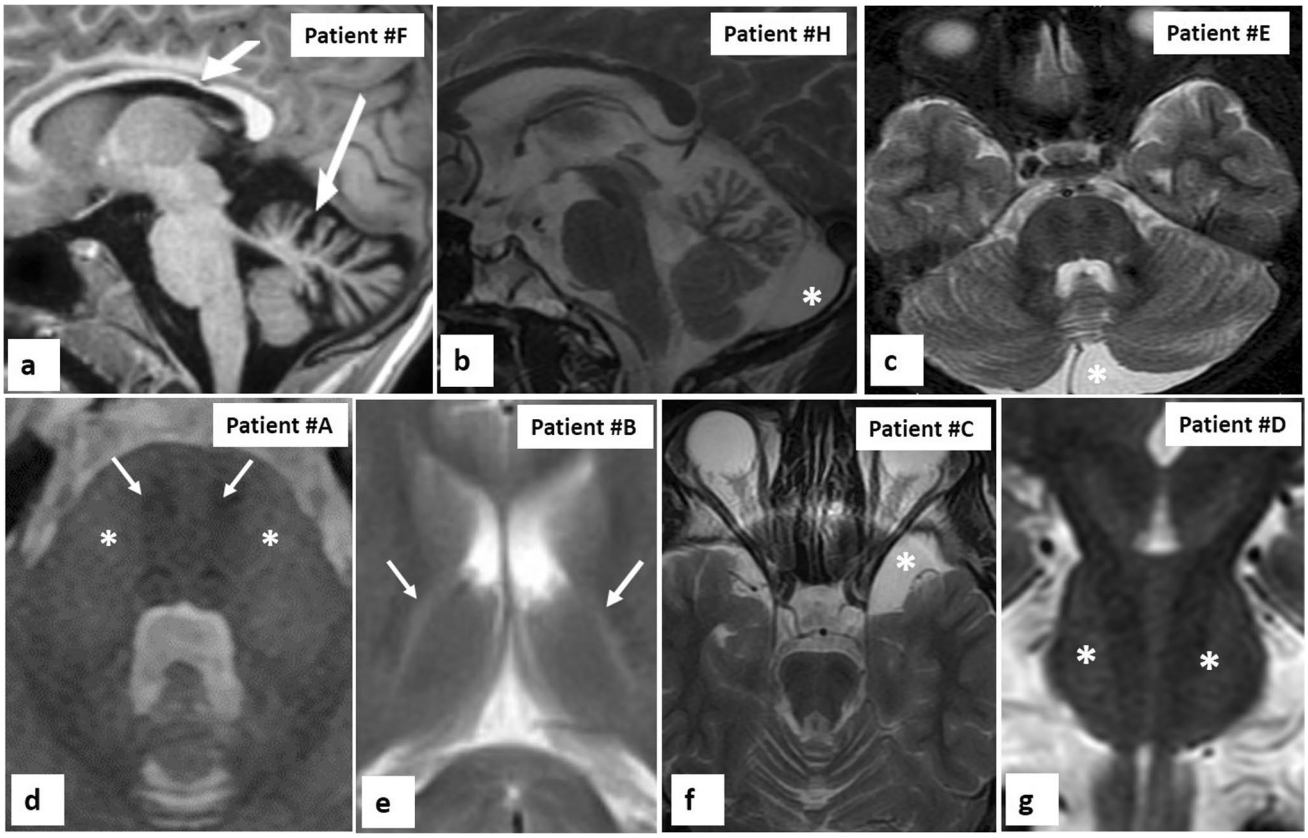

Fig. 2 Significant MRI findings in ARSACS patients. **a** Thinning of the posterior mid-body of the corpus callosum (short thick arrow) as well as the superior cerebellar vermis atrophy (long thin arrow) in patient F (*SACS*: *c.3427C>T*). **b** Posterior fossa arachnoid cyst (asterisk) in patient H (*SACS: c.7504C>T*). **c** Asymmetry of the posterior fossa (asterisk) in patient E (*SACS: c.3281dupA*). **d** Pontine stripes (arrow) as well as thickening of the middle cerebellar peduncle (asterisk) in patient A (*SACS: c.10813A>T*). **e** Hyperintense thalamus rim (arrow) in patient E (*SACS: c.3281dupA*). **f** Temporal arachnoid cyst (asterisk) in patient C (*SACS: c.8132C>A*). **g** Hyperintensity of lateral of pons (asterisk) in patient D (*SACS:* c.2439_2440delAT)

consecutive early-onset ataxia cohort detected a lower frequency of ARSACS (5%) in the Western Europe populations [2]. Of note, the slightly higher relative prevalence of ARSACS in this study might be explained by the higher rate of consanguineous marriage in Iran, which increases the likelihood of autosomal recessive rare Mendelian

Table 3 Features of the identified variant based on online databases

Patient ID	Variant coordinates SACS (NM_014363.6)	Zygosity	In silico parameters	References	Allele frequencies[1]	Type and classification[2]
A	Chr13(hg38):g 23,333,063 c.10813A > T (p.Lys3605Ter) Exon 10/10	Homozygous	MutationTaster: disease causing FATHMM-MKL: damaging EIGEN: pathogenic	Not reported	gnomAD: NA ExAC: NA Iranome: NA	Nonsense Pathogenic (Class 1)
B	Chr13(hg38):g 23,334,010 c.9866C > G (p.Ser3289Ter) Exon 10/10	Homozygous	MutationTaster: disease causing FATHMM-MKL: damaging EIGEN: pathogenic	Not reported	gnomAD: NA ExAC: NA Iranome: NA	Nonsense Pathogenic (Class 1)
C	Chr13(hg38):g 23,335,744 c.8132C > A (p.Ser2711Ter) Exon 10/10	Homozygous	MutationTaster: disease causing FATHMM-MKL: damaging EIGEN: pathogenic	Not reported	gnomAD: NA ExAC: NA Iranome: NA	Nonsense Pathogenic (Class 1)
D	Chr13(hg38):g 23,341,436 c.2439_2440delAT (p.Val815GlyfsTer4) Exon 10/10	Homozygous	MutationTaster: NA FATHMM-MKL: NA EIGEN: NA	Reported (PMID: 23,043,354)	gnomAD: 0.00003943 ExAC: 0.000008243 Iranome: NA	Frameshift deletion Pathogenic (Class 1)
E, I	Chr13(hg38):g 23,340,595 c.3281dupA (p.Asn1094LysfsTer18) Exon 10/10	Homozygous	MutationTaster: NA FATHMM-MKL: NA EIGEN: NA	Not reported	gnomAD: NA ExAC: NA Iranome: NA	Frameshift insertion Pathogenic (Class 1)
F	Chr13(hg38):g 23,340,449 c.3427C > T (p.Gln1143Ter) Exon 10/10	Homozygous	MutationTaster: disease causing FATHMM-MKL: damaging EIGEN: pathogenic	Not reported	gnomAD: NA ExAC: NA Iranome: NA	Nonsense Pathogenic (Class 1)
G	Chr13(hg38):g 23,335,160 c.8716C > T (p.Arg2906Ter) Exon 10/10	Homozygous	MutationTaster: disease causing FATHMM-MKL: damaging EIGEN: pathogenic	Not reported	gnomAD: 0.00001974 ExAC: 0.00001651 Iranome: NA	Nonsense Pathogenic (Class 1)
H	Chr13(hg38):g 23,336,372 c.7504C > T (p.Arg2502Ter) Exon 10/10	Homozygous	MutationTaster: disease causing FATHMM-MKL: damaging EIGEN: pathogenic	Reported (PMIDs: 32,368,540, 26,693,535, 23,280,630, 28,658,401, 23,250,129)	gnomAD: NA ExAC: 0.000008240 Iranome: NA	Nonsense Pathogenic (Class 1)
J	Chr13(hg38):g 23,340,183 c.3695_3697del (p.Val1232del) Exon 10/10	Homozygous	MutationTaster: NA FATHMM-MKL: NA EIGEN: NA	Not reported	gnomAD: NA ExAC: NA Iranome: NA	Inframe deletion VUS (Class 3)

[1]Genome Aggregation Database (gnomAD) Genome version: 3.1.2, Exome Aggregation Consortium (ExAC) version: 1.0 and Iranome

[2]Variant classification is based on ACMG recommendations: class 1, pathogenic; class 2, likely pathogenic; class 3, variant of uncertain significance (VUS); class 4, likely benign; class 5, benign

disorders in an inbreed population of patients with early-onset ataxia [19]. The mean age of disease onset was 5.6 years (range, 1–11 years). Regardless of earlier age of disease onset that has been reported among original cases of ARSACS in Quebec, a wide variety of disease onset has been reported from infancy through adulthood. An overall mean age of disease onset has been delineated as 3 years old [4, 20].

The classic clinical triad of ARSACS including ataxia, neuropathy, and pyramidal tract involvement was present in 80% (8/10) of our patients. All cases manifested with both ataxia and neuropathy; however, only half of them showed

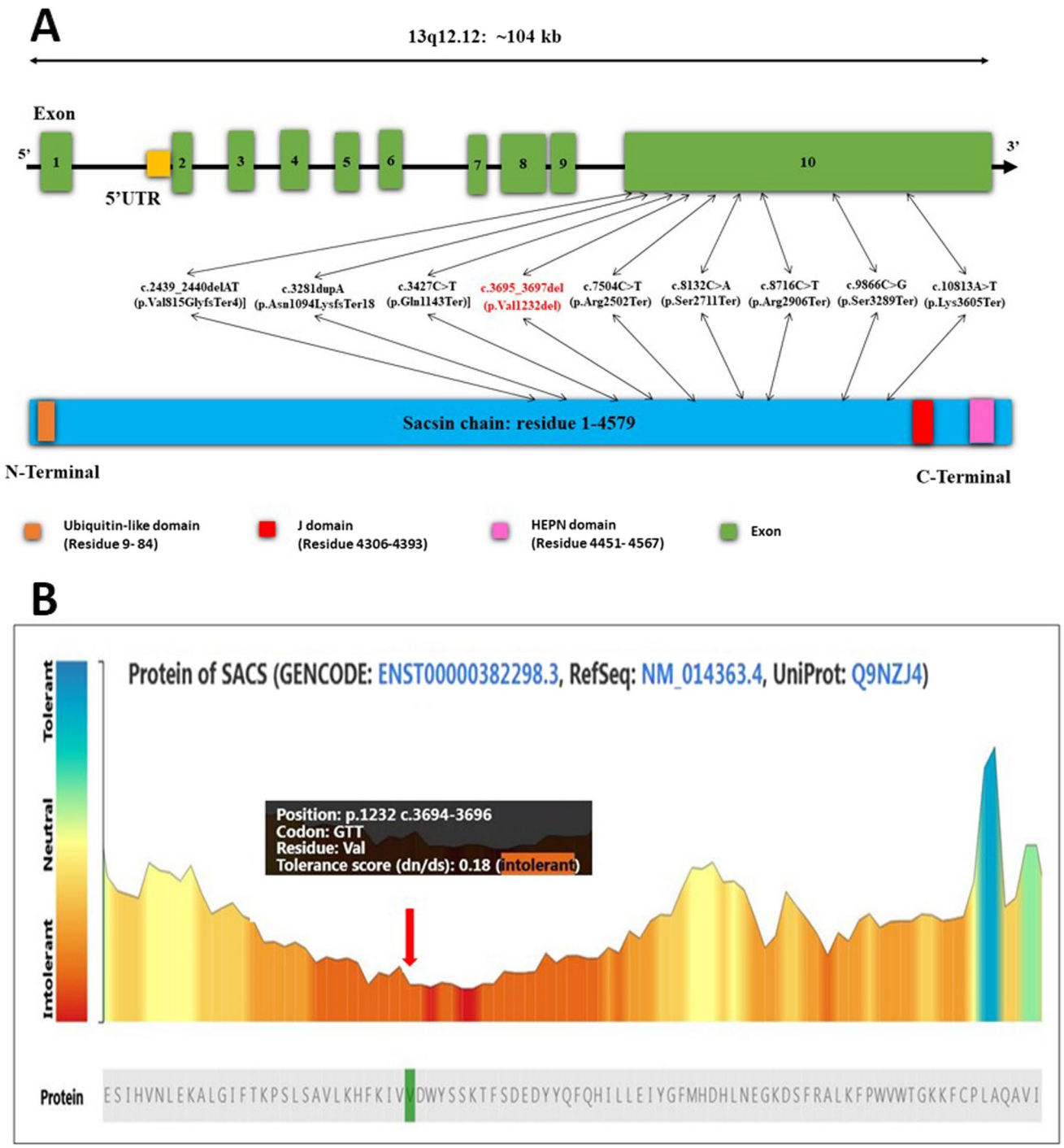

Fig. 3 **A** The *SACS* gene contains ten exons and spans ~ 104 kb. Graphical view of the Sacsin protein (UniProtKB, Q9NZJ4) updated from UniProt (https://www.uniprot.org/uniprot/Q9NZJ4). The canonical isoform length of the Sacsin protein (identifier: Q9NZJ4-1) is 4579 amino acids and contains three functional domains, including ubiquitin-like domain (UBL) (residue 9–84), J domain (residue 4306–4393), and HEPN domain (residue 4451–4567). All identified variants are in the exon 10 of *SACS* gene, including eight pathogenic variants shown in black and one VUS variant shown in red. **B** MetaDome server (https://stuart.radboudumc.nl/metadome) was used to identify the intolerant regions in the sacsin protein. As shown by the red arrow, Val1232 is located in a highly intolerant region of the protein

upward plantar reflex. Of note, peripheral neuropathy can leave the pyramidal features undiagnosed. These clinical findings were as frequent as other studies [4]. However, the presence of all three typical clinical features is not mandatory for making the diagnosis. Lower limb spasticity was detected in 6/10 patients (60%). Given that pyramidal tract

involvement may not be limited to the lower limbs, upper limbs spasticity was detected in one patient of ours [2]. No urinary problems, school performance failure, hearing impairment, or dysphagia was reported among our patients (Table 1). These complicating features are by far not as frequent as the typical triad of the disease as intellectual disability, hearing abnormality, and urinary dysfunction have been reported in 11.4%, 3.3%, and 8.6% of patients [4]. Assessment of such complicating features with quantitative scales can lead to improve the quality of life of patients by addressing them properly.

Nerve conduction studies revealed chronic sensorimotor polyneuropathy in all 10 patients. Half of them showed chronic demyelinating sensorimotor polyneuropathy with secondary axonal degeneration, while the remaining had pure axonal sensorimotor polyneuropathy with no evidence of demyelination features. In Pilliod J et al. study, 25% of patients had axonal type neuropathy, while 53% of cases had demyelinating neuropathy [21]. In late-onset ARSACS that usually manifests after 40 years old, neuropathy may be obscure in the early stages of the disease; therefore, the absence of neuropathic changes cannot rule out the diagnosis in suspected cases [2].

Atrophy of superior cerebellar vermis and pontine stripes was universal MRI findings in all our patients. These imaging findings are in line with Synofzik et al. study of patients with unexplained early-onset ataxia consisting 11 index cases with ARSACS in 2013 [2] but higher than a systematic review of 222 patients with this disorder (60.8% and 33.3%, respectively) [4]. The lack of consistency in imaging findings could be explained in part because of overlooking the pontine stripes on brain MRI. Of note, MRI tractography in ARSACS has shown that these "pontine stripes" correspond to partly displaced and thickened transverse pontine fibers. In addition, on brain MR spectroscopy, these thickened transverse pontine fibers show increased fractional anisotropy (FA), decreased radial diffusivity (RD), and increased axial diffusivity (AD), suggesting a likely hypertrophy and/or hypermyelination of these fibers [22]. Bilateral hyperintensity of the lateral side of the pons in coronal T2-w and hyperintense rim surrounding both thalami in T2-w images was also detected in 8/10 and 9/10 of patients, respectively. Thinning of the posterior mid-body portion of the corpus callosum was detected in 70% (7/10) of our cases that was showing a comparable frequency seen in Synofzik et al. cohort [2].

Arachnoid cyst accounts for 1–2% of intracranial imaging findings. In pediatric population, it can be detected in up to 2.6% of neuroimaging findings [22–24]. Posterior fossa arachnoid cysts were reported in 75% and 54% of ARSACS patients in Synofzik et al. and Rezende Filho et al. reports, respectively [2, 25]. Posterior fossa arachnoid cysts were detected in half of our cases (50%), while it was detected in anterior temporal region in 2 patients (20%). Indeed, anterior temporal arachnoid cyst was detected as a novel associated imaging finding in a cohort of ARSACS patients.

All nine individual sequence variants were identified in this study located in the exon 10 of *SACS* gene, which is the longest exon of the *SACS* and encodes 3850 amino acids. Eight of these nine variants were pathogenic, including six nonsense, one frameshift deletion, and one frameshift insertion, which was shared between two patients. These 8 variants result in the production of a truncated protein and loss of downstream functional domains including J and HEPN domains (Fig. 3A). Given that these pathogenic variants occurred in the last exon of the *SACS* gene, nonsense-mediated decay (NMD) as one of the surveillance mechanisms of the RNA cannot recognize them [26]. The identified frameshift deletion variant was reported previously [27]. In addition, seizure, mental retardation, and hammer toe deformity were reported with this variant in the Hammer's study, but our patient had none of these symptoms [27].

Notably, a rare novel homozygous inframe deletion variant, [NM_014363.6: c.3695_3697del; (p.Val1232del)], was identified in exon 10 of the *SACS* in one of our patients. This variant is classified as VUS based on ACMG guideline and was not found in the genomic projects. Evolutionary conservation analysis was performed by use of the UCSC genome browser (https://genome.ucsc.edu/), which showed that Val at residue 1232 of the *SACS* has been conserved during the evolution between different species including rhesus, mouse, dog, zebrafish, elephant, x-tropicalis, and chicken, which indicates that this amino acid is essential for the normal functioning of the protein. Also, the I-Mutant2.0 server, which computes the $\Delta\Delta G$ values of protein variant, was utilized to predict the effect of the (p.Val1232del) variant on protein stability. This analysis showed that all missense variants in the Val1232 of the sacsin protein have negative $\Delta\Delta G$; therefore, any change in this amino acid reduces the stability of the protein ($\Delta\Delta G < 0$, decrease stability). The intolerant regions in the sacsin protein were analyzed by MetaDome server; Val1232 was located in a highly intolerant region; therefore, deletion of this amino acid may have an intolerable effect on the protein structure that is in favor of pathogenicity of this variant (Fig. 3B).

The study had some limitations. Patients were initially diagnosed based on their clinical phenotype followed which met the molecular diagnosis by genetic tests. Optical coherence tomography (OCT) to evaluate the retinal nerve fiber layer thickness has been suggested as a useful diagnostic tool especially in atypical cases of ARSACS [18], but it was not performed in our patients. The small number of patients with ARSACS is another limitation of this study; however, international collaboration multinational cohort studies can overcome this issue and better understanding of the natural history of ARSACS.

Conclusion

The findings of this study support the relatively notable prevalence of ARSACS among patients with early-onset ataxia including non-Quebec populations. Furthermore, this study extends the neuroimaging phenotype of ARSACS by demonstrating anterior temporal arachnoid cyst in two patients and the genotype landscape of the disease by presenting 8 pathogenic and one VUS variants, which 7 of them have not been reported previously.

Supplementary Information The online version contains supplementary material available at https://doi.org/10.1007/s12311-022-01430-3.

Acknowledgements The authors thank all participant families and their patients in this research. The authors are especially thankful to Ali Mohebi and Nahid Vafaee from the Growth and Development Research Center, Tehran University of Medical Sciences, for their support in data gathering. The authors thank the Hertie Institute for Clinical Brain Research, Tübingen, Germany, as the international collaborative party of the study.

Author Contribution MRA and MH designed and supervised the study. ZR, ART, PM, and NM had a major contribution in drafting the manuscript. ZR, MH, ART, SH, MR, MR, RAM, RSB, DF, AZD, and AR interpreted clinical data. ART and MS contributed in the final scientific revision. NM, PM, and SS contributed in genetic data analyses. MGA interpreted the electrodiagnostic data. All authors reviewed and approved the final manuscript.

Funding This project was supported by the Deutsche Forschungsgemeinschaft (DFG) (German Research Foundation) No. 441409627, as part of the PROSPAX consortium under the frame of EJP RD, the European Joint Programme on Rare Diseases, under the EJP RD COFUND-EJP N° 825575. This study was granted by NIMAD under the proposal No. 971846.

Data Availability Human variants and pertinent phenotypes have been reported to ClinVar (Submission IDs: SUB9677044, SUB9677045, SUB9677050, SUB9677685, SUB9677710, SUB9677755, SUB9677767, SUB9677775).

Declarations

Ethics Approval This study was approved by the ethics committee of the National Institute for Medical Research Development of Iran (Ethics ID: IR.NIMAD.REC.1397.508) and has thus been performed in accordance with the ethical standards laid down in the 1964 Declaration of Helsinki and its later amendments.

Consent to Participate Informed consent was obtained from all individual participants enrolled in the study.

Consent for Publication Participant families agreed on anonymous publication of patients' clinical information and their relevant data.

Competing Interests The authors declare no competing interests.

References

1. Vermeer S, Meijer RP, Pijl BJ, Timmermans J, Cruysberg JR, Bos MM, et al. ARSACS in the Dutch population: a frequent cause of early-onset cerebellar ataxia. Neurogenetics. 2008;9(3):207–14.
2. Synofzik M, Soehn AS, Gburek-Augustat J, Schicks J, Karle KN, Schüle R, et al. Autosomal recessive spastic ataxia of Charlevoix Saguenay (ARSACS): expanding the genetic, clinical and imaging spectrum. Orphanet J Rare Dis. 2013;8(1):1–13.
3. Synofzik M, Nemeth AH. Recessive ataxias. Handb Clin Neurol. 2018;155:73–89.
4. Xiromerisiou G, Dadouli K, Marogianni C, Provatas A, Ntellas P, Rikos D, et al. A novel homozygous SACS mutation identified by whole exome sequencing-genotype phenotype correlations of all published cases. J Mol Neurosci. 2020;70(1):131–41.
5. Habibzadeh P, Tabatabaei Z, Inaloo S, Nashatizadeh MM, Synofzik M, Ostovan VR, et al. Case report: expanding the genetic and phenotypic spectrum of autosomal recessive spastic ataxia of Charlevoix-Saguenay. Front Genet. 2020;11:585136.
6. Artero Castro A, Machuca C, Rodriguez Jimenez FJ, Jendelova P, Erceg S. Short review: investigating ARSACS: models for understanding cerebellar degeneration. Neuropathol Appl Neurobiol. 2019;45(6):531–7.
7. Parfitt DA, Michael GJ, Vermeulen EG, Prodromou NV, Webb TR, Gallo J-M, et al. The ataxia protein sacsin is a functional co-chaperone that protects against polyglutamine-expanded ataxin-1. Hum Mol Genet. 2009;18(9):1556–65.
8. Becker EB, Oliver PL, Glitsch MD, Banks GT, Achilli F, Hardy A, et al. A point mutation in TRPC3 causes abnormal Purkinje cell development and cerebellar ataxia in moonwalker mice. Proc Natl Acad Sci USA. 2009;106(16):6706–11.
9. Breckpot J, Takiyama Y, Thienpont B, Van Vooren S, Vermeesch JR, Ortibus E, et al. A novel genomic disorder: a deletion of the SACS gene leading to spastic ataxia of Charlevoix-Saguenay. Eur J Hum Genet. 2008;16(9):1050–4.
10. Richards S, Aziz N, Bale S, Bick D, Das S, Gastier-Foster J, et al. Standards and guidelines for the interpretation of sequence variants: a joint consensus recommendation of the American College of Medical Genetics and Genomics and the Association for Molecular Pathology. Genetics in medicine. 2015;17(5):405–23.
11. Mohammadi P, Heidari M, Ashrafi MR, Mahdieh N, Garshasbi MG. A novel homozygous missense variant in the NAXE gene in an Iranian family with progressive encephalopathy with brain edema and leukoencephalopathy. Acta Neurol Belg. 2021. https://doi.org/10.1007/s13760-021-01717-y.
12. Mohammadi P, Salehi Siavashani E, Mohammadi MF, Bahramy A, Almadani N, Garshasbi MG. Whole-exome sequencing identified first homozygous frameshift variant in the COLEC10 gene in an Iranian patient causing 3MC syndrome type 3. Mol Genet Genomic Med. 2021;9:e1834.
13. Chen S, Zhou Y, Chen Y, Gu J. fastp: an ultra-fast all-in-one FASTQ preprocessor. Bioinformatics. 2018;34(17):i884–90.
14. Abuín JM, Pichel JC, Pena TF, Amigo J. BigBWA: approaching the Burrows-Wheeler aligner to Big Data technologies. Bioinformatics. 2015;31(24):4003–5.
15. Fattahi Z, Beheshtian M, Mohseni M, Poustchi H, Sellars E, Nezhadi SH, et al. Iranome: a catalogue of genomic variations in the Iranian population. Hum Mutat. 2019;40(11):1968–84.
16. Schwarz JM, Cooper DN, Schuelke M, Seelow D. MutationTaster2: mutation prediction for the deep-sequencing age. Nat Methods. 2014;11(4):361–2.
17. Shihab HA, Rogers MF, Gough J, Mort M, Cooper DN, Day IN, et al. An integrative approach to predicting the functional effects

of non-coding and coding sequence variation. Bioinformatics. 2015;31(10):1536–43.
18. Parkinson MH, Bartmann AP, Clayton LM, Nethisinghe S, Pfundt R, Chapple JP, et al. Optical coherence tomography in autosomal recessive spastic ataxia of Charlevoix-Saguenay. Brain. 2018;141(4):989–99.
19. Hosseini-Chavoshi M, Abbasi-Shavazi MJ, Bittles AH. Consanguineous marriage, reproductive behaviour and postnatal mortality in contemporary Iran. Hum Hered. 2014;77(1–4):16–25.
20. Engert JC, Doré C, Mercier J, Ge B, Bétard C, Rioux JD, et al. Autosomal recessive spastic ataxia of Charlevoix-Saguenay (ARSACS): high-resolution physical and transcript map of the candidate region in chromosome region 13q11. Genomics. 1999;62(2):156–64.
21. Pilliod J, Moutton S, Lavie J, Maurat E, Hubert C, Bellance N, et al. New practical definitions for the diagnosis of autosomal recessive spastic ataxia of Charlevoix-Saguenay. Ann Neurol. 2015;78(6):871–86.
22. Oguz K, Haliloglu G, Temucin C, Gocmen R, Has A, Doerschner K, et al. Assessment of whole-brain white matter by DTI in autosomal recessive spastic ataxia of Charlevoix-Saguenay. Am J Neuroradiol. 2013;34(10):1952–7.
23. Chan JL, Tan AL, Ng LP, Low DC, Tew SW, Low SY. Paediatric arachnoid cysts: surgical outcomes from a Singapore children's hospital. J Clin Neurosci. 2021;85:122–31.
24. Dlaka D, Raguž M, Muller D, Romić D, Almahariq F, Dlaka J, et al. Intraparenchymal supratentorial arachnoid cyst: a case report. Egypt J Neurosurg. 2019;34(1):1–6.
25. Rezende Filho FM, Parkinson MH, Pedroso JL, Poh R, Faber I, Lourenço CM, et al. Clinical, ophthalmological, imaging and genetic features in Brazilian patients with ARSACS. Parkinsonism Relate Disord. 2019;62:148–55.
26. Chang Y-F, Imam JS, Wilkinson MF. The nonsense-mediated decay RNA surveillance pathway. Annu Rev Biochem. 2007;76:51–74.
27. Hammer MB, Eleuch-Fayache G, Gibbs JR, Arepalli SK, Chong SB, Sassi C, et al. Exome sequencing: an efficient diagnostic tool for complex neurodegenerative disorders. Eur J neurol. 2013;20(3):486–92.

Authors and Affiliations

Mahmoud Reza Ashrafi[1,2] · Pouria Mohammadi[1,3] · Ali Reza Tavasoli[1,4,5] · Morteza Heidari[1,4] · Sareh Hosseinpour[1,6] · Maryam Rasulinejad[1] · Mohammad Rohani[7] · Masoud Ghahvechi Akbari[1,8] · Reza Azizi Malamiri[9] · Reza Shervin Badv[1] · Davood Fathi[10,11] · Ali Zare Dehnavi[1] · Shahram Savad[12] · Ali Rabbani[1,2] · Matthis Synofzik[13,14] · Nejat Mahdieh[15] · Zahra Rezaei[1]

1 Pediatric Neurology Division, Children's Medical Center, Pediatrics Center of Excellence, Ataxia Clinic, Tehran University of Medical Sciences, Tehran, Iran

2 Department of Pediatrics Center, Growth and Development Research Center, Pediatrics Center of Excellence, Tehran University of Medical Sciences, Tehran, Iran

3 Faculty of Medical Sciences, Department of Medical Genetics, Tarbiat Modares University, Tehran, Iran

4 Pediatric Neurology Division, Children's Medical Center, Pediatrics Center of Excellence, Myelin Disorders Clinic, Tehran University of Medical Sciences, Tehran, Iran

5 Jefferson Institute of Molecular Medicine, Thomas Jefferson University, Philadelphia, USA

6 Department of Pediatric Neurology, Vali-E-Asr Hospital, Imam Khomeini Hospital Complex, Tehran University of Medical Sciences, Tehran, Iran

7 Department of Neurology, School of Medicine, Hazrat Rasool-E Akram General Hospital, Iran University of Medical Sciences, Tehran, Iran

8 Physical Medicine and Rehabilitation Department, Children's Medical Center, Tehran University of Medical Sciences, Tehran, Iran

9 Division of Pediatric Neurology, Department of Pediatrics, Golestan Medical, Educational and Research Center, Ahvaz Jundishapour University of Medical Sciences, Ahvaz, Iran

10 Brain and Spinal Cord Injury Research Center, Neuroscience Institute, Tehran University of Medical Sciences, Tehran, Iran

11 Neurology Department, Shariati Hospital, Tehran University of Medical Sciences, Tehran, Iran

12 Department of Medical Genetics, Tehran University of Medical Sciences, Tehran, Iran

13 Division Translational Genomics of Neurodegenerative Diseases, Hertie-Institute for Clinical Brain Research and Center of Neurology, University of Tübingen, Tübingen, Germany

14 Center for Neurodegenerative Diseases (DZNE), Tübingen, Germany

15 Cardiogenetic Research Center, Rajaei Cardiovascular Medical and Research Center, Iran University of Medical Sciences, Tehran, Iran